Supplementary Information

Energizing Hybrid Supercapacitor by Using Mn^{2+}-Based Active Electrolyte

Lei Yan, Jianhang Huang, Xiaoli Dong, Zhaowei Guo, Zhuo Wang, Yonggang Wang*

Department of Chemistry and Shanghai Key Laboratory of Molecular Catalysis and Innovative Materials, Institute of New Energy, iChEM (Collaborative Innovation Center of Chemistry for Energy Materials) Fudan University, Shanghai 200433, China.

*E-mail: ygwang@fudan.edu.cn

Capacitance calculation

The specific capacitance (F g^{-1}) of the galvanostatic charge-discharge performance was calculated through the following equation:

$$C = \frac{It}{m\Delta E}$$

Where C (F g^{-1}), I (A), ΔE (V), t (s), and m (g) denote the specific capacitance, constant discharge current, the voltage change after a full discharge process, the time period for a full discharge, and the mass of active materials, respectively.

Calculations about energy density and power density of the hybrid supercapacitor

The energy density and powder density of hybrid supercapacitor were calculated by following equations:

$$E_{\mathrm{g}} = \frac{\int IV_{(t)}d_t}{3.6m} = \frac{I}{3.6m}\int V_{(t)}d_t$$

$$P_{\mathrm{g}} = \frac{E_g \times 3600}{\Delta t}$$

Herein, E_g represents the energy density (Wh kg^{-1}), P represents the power density (W kg^{-1}). $V_{(t)}$ is discharging voltage at t, m is the total mass of 400-KOH-Ti_3C_2 and consumed MnO_2. d_t is time differential, the value of $\int Vd$ could be calculated from discharge portion of galvanostatic charge/discharge curves.

Calculation about ionic conductivity of the electrolyte

The ionic conductivity of the electrolyte at -70 ^{o}C was calculated by following equation:

$$\sigma = \frac{l}{A \times R}$$

Herein, σ represents the ionic conductivity of electrolyte (mS cm^{-1}). L is the interval distance between the Ti-plate electrodes (cm). A is the area of Ti-plate electrode (cm^{-2}). R is the resistance of electrolyte (Ohm).

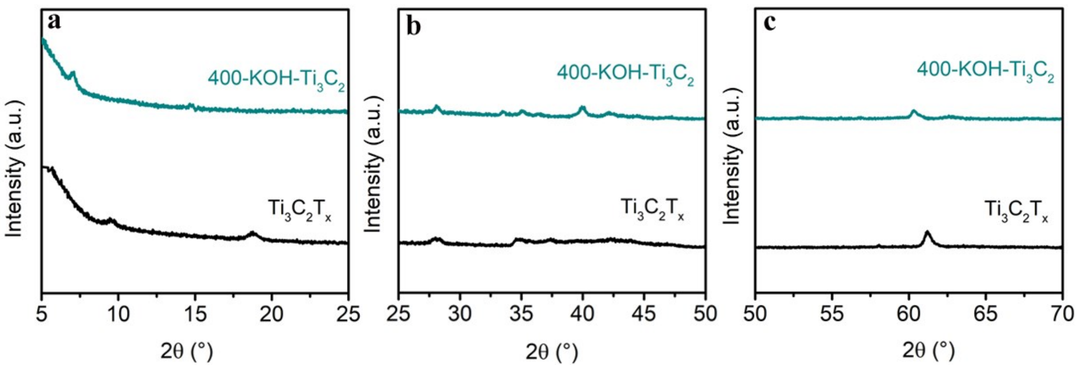

Figure S1. (a-c) The enlarged view of the XRD pattern for 400-KOH-Ti_3C_2.

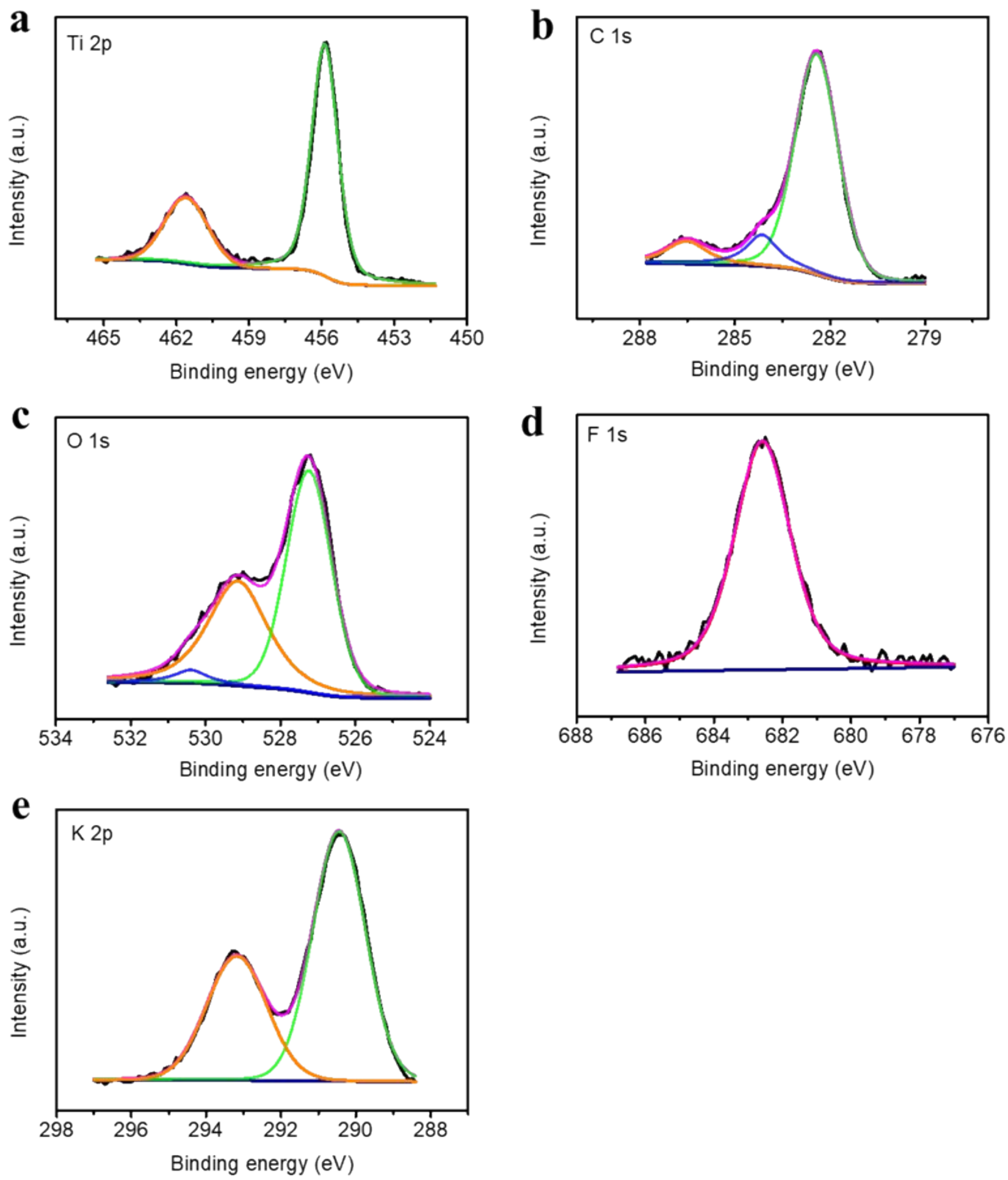

Figure S2. High-resolution XPS spectra of 400-KOH-Ti_3C_2 in the Ti 2p (a), C 1s (b), O 1s (c), F 1s (d) and K 2p (e) regions.

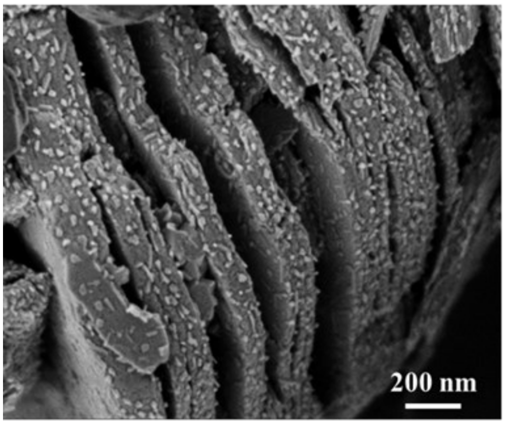

Figure S3. The SEM image of the 400-KOH-Ti_3C_2 sample.

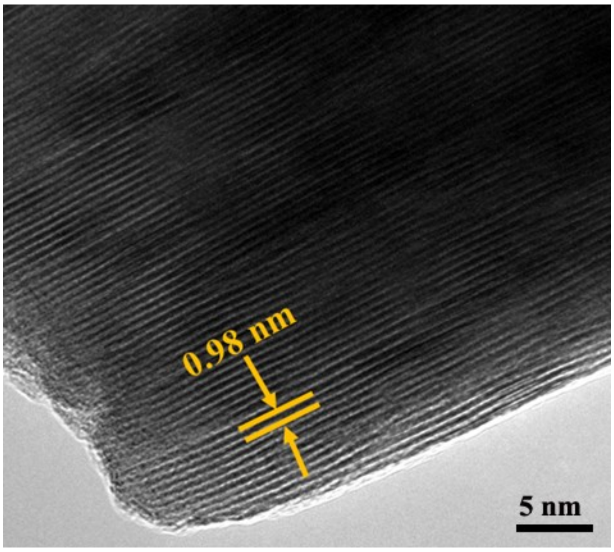

Figure S4. The high-resolution TEM image of original $Ti_3C_2T_x$.

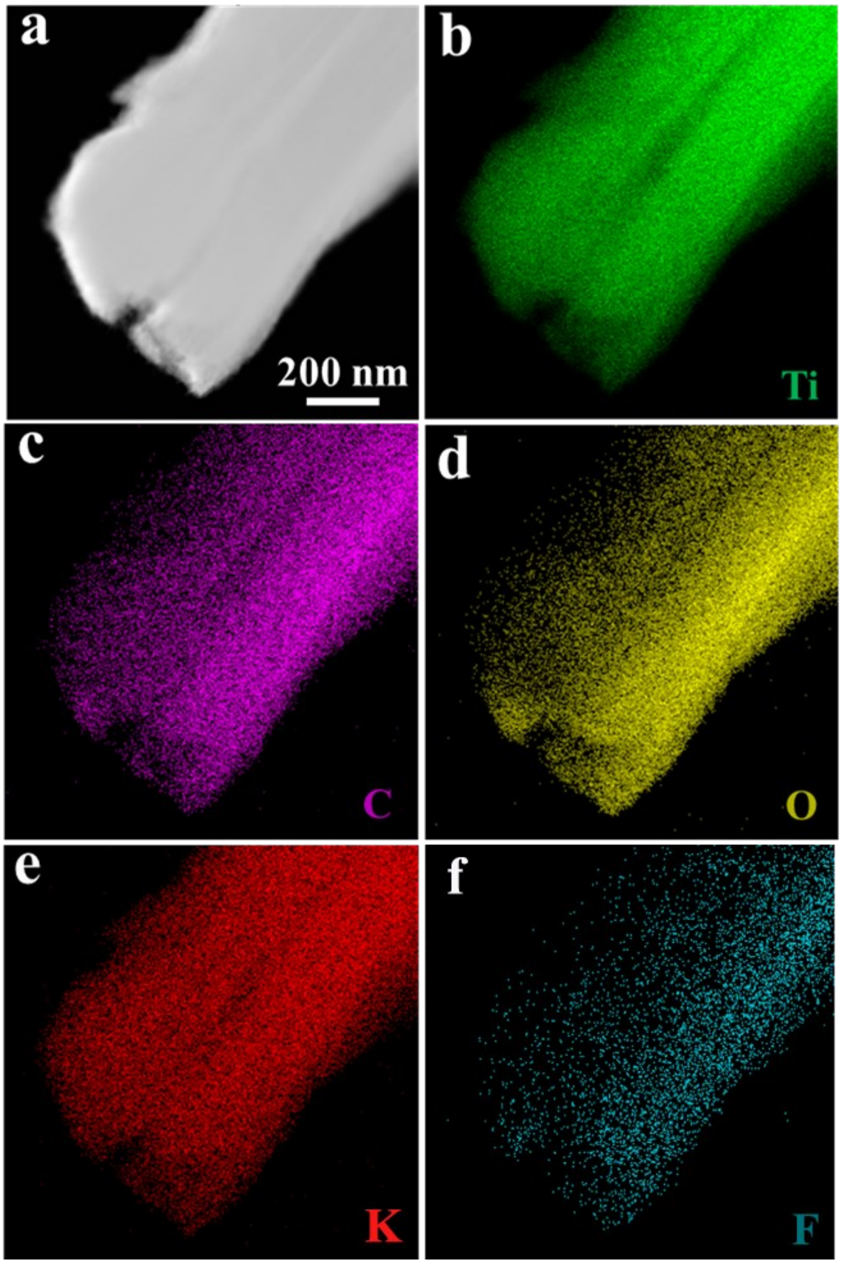

Figure S5. EDX element mapping images of 400-KOH-Ti_3C_2.

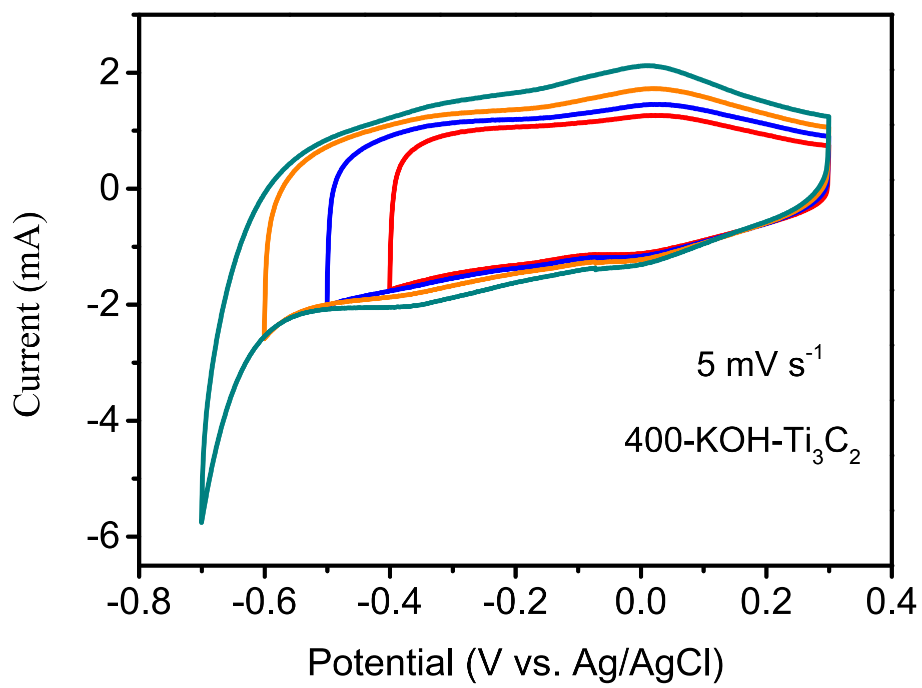

Figure S6. The CV curves of 400-KOH-Ti_3C_2 anode in different potential windows of −0.4 to 0.3, −0.5 to 0.3, −0.6 to 0.3 and −0.7 to 0.3 V at a same scan rate of 5 mV s^{-1}.

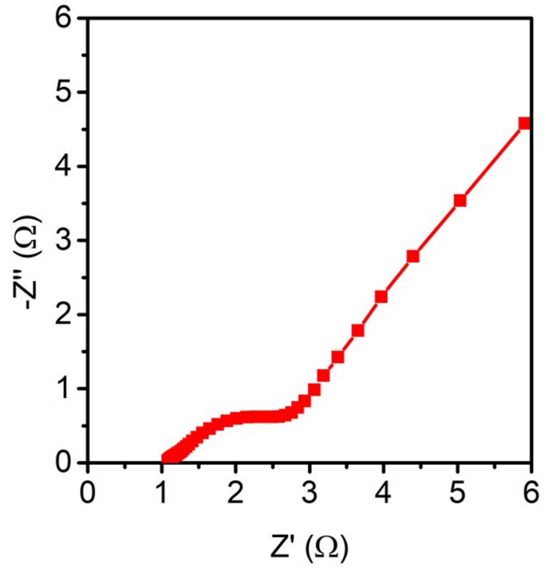

Figure S7. Nyquist plot of the original $Ti_3C_2T_x$.

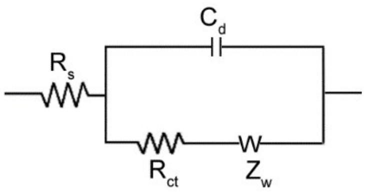

Figure S8. The equivalent circuit adopted in the simulation of EIS spectra of 400-KOH-Ti_3C_2 electrode.

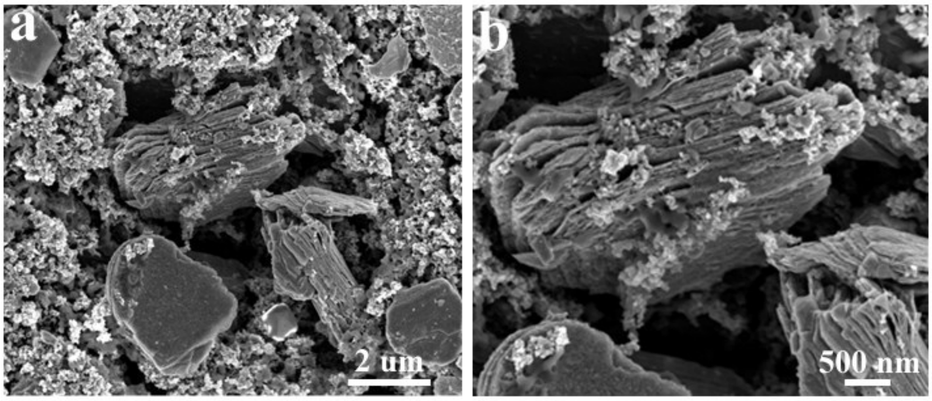

Figure S9. (a, b) SEM images of 400-KOH-Ti_3C_2 electrode after 5000 cycles.

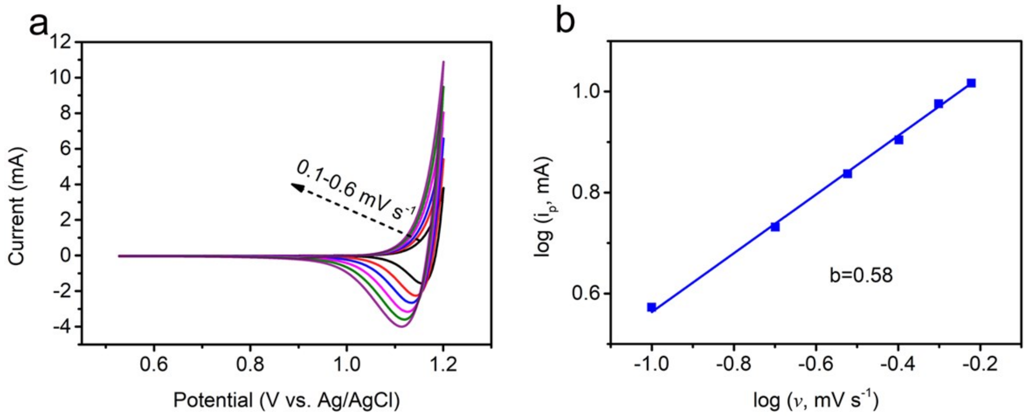

Figure S10. (a) CV curves of CF-electrode at various scan rates in 2 M H_2SO_4 + 2 M $MnSO_4$ solution. (b) Relationship between the peak current and scan rate of the CF-electrode. The b-value is 0.58, indicating the fast reaction kinetics of Mn^{2+}/MnO_2 deposition/dissolution.

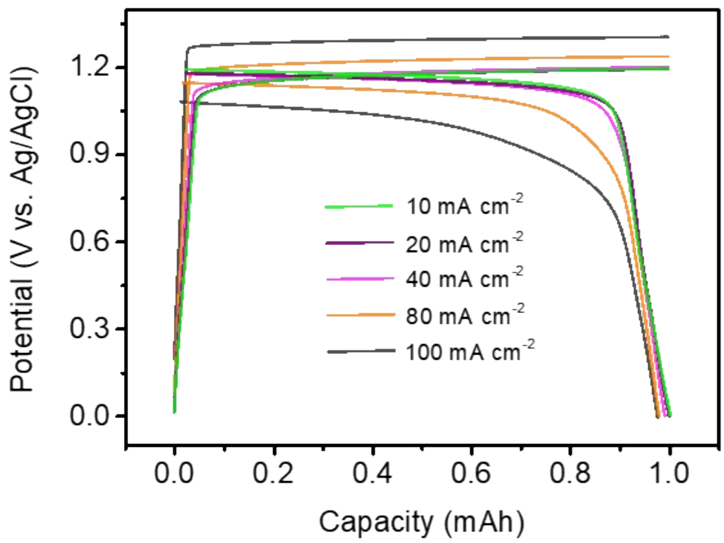

Figure S11. The galvanostatic charge/discharge curves of CF electrode in the acid electrolyte containing Mn^{2+} with the deposition capacity of 1 mAh at different current densities.

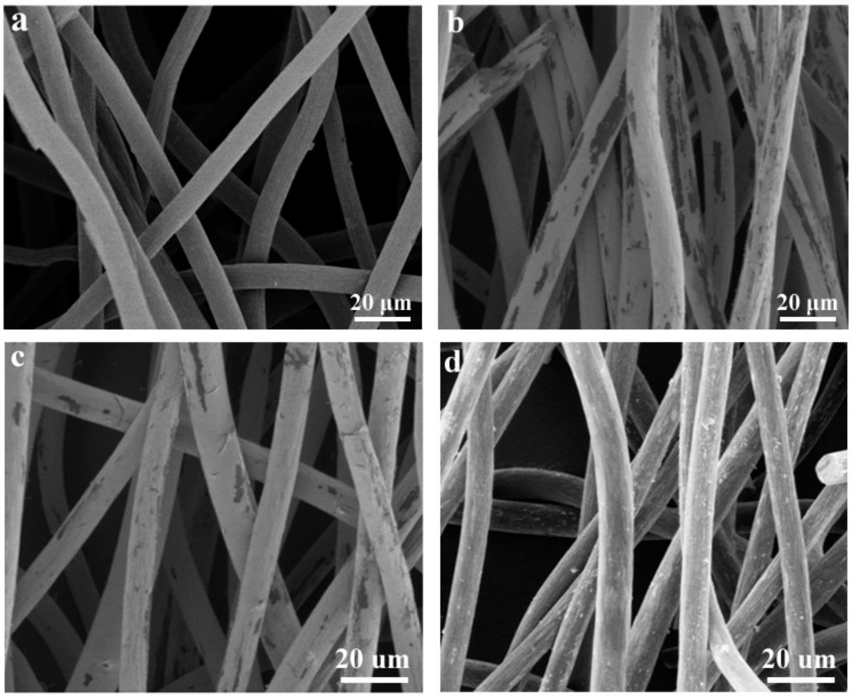

Figure S12. (a) SEM image of initial CF electrode. (b) SEM image of MnO_2@CF electrode. (c) SEM image of the CF electrode after the 5000th charge at 1.2 V to 1 mAh cm^{-2}. (d) SEM image of the CF electrode after the 5000th discharge at 40 mA cm^{-2} to 0.5 V.

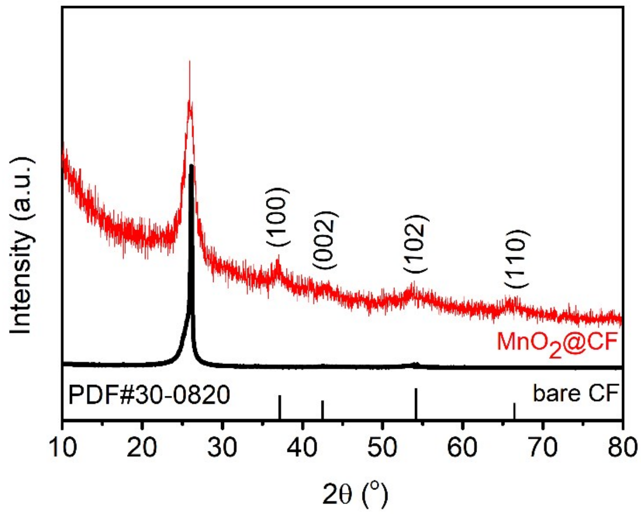

Figure S13. XRD patterns of the pristine CF and MnO_2@CF.

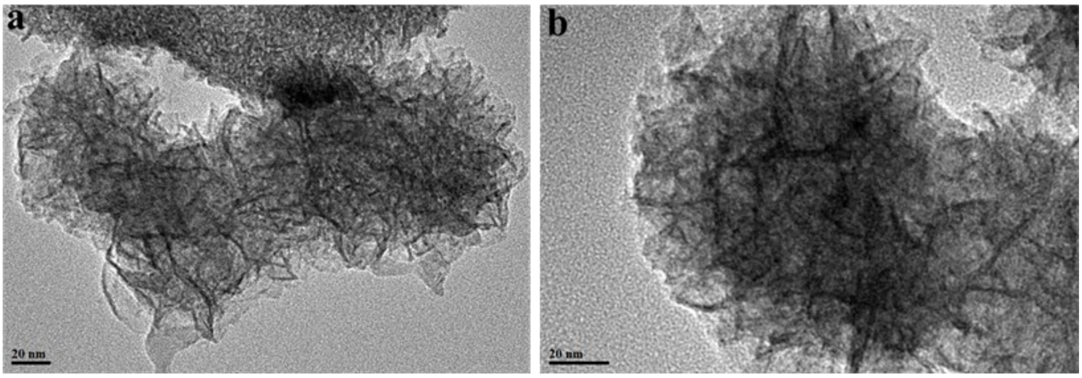

Figure S14. The TEM images of deposited MnO_2.

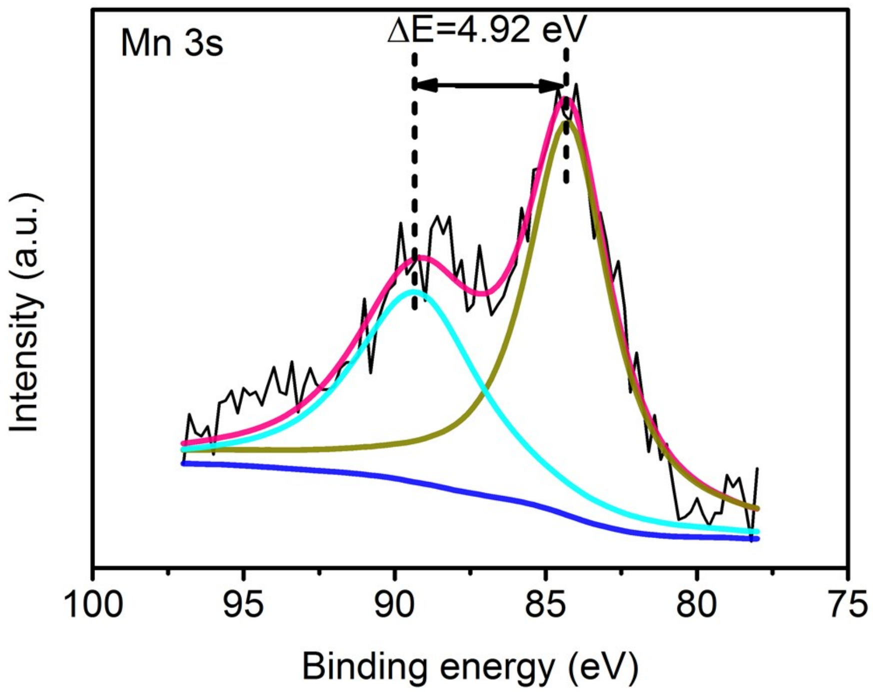

Figure S15. High-resolution Mn 3s XPS spectra of deposited MnO_2.

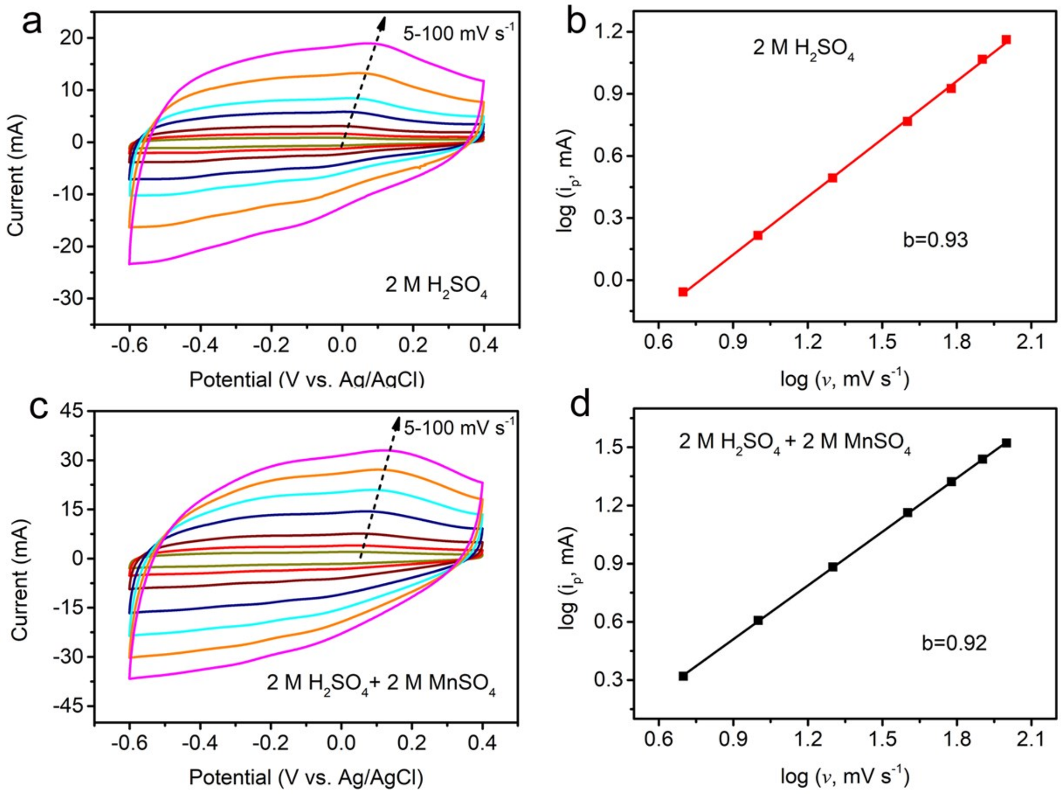

Figure S16. CV curves of the 400-KOH-Ti_3C_2 electrodes at various scan rates in 2 M H_2SO_4 solution and 2 M H_2SO_4 + 2 M $MnSO_4$ solution (a, c) and the corresponding relationship between the peak current and scan rate (b, d). The peak current (i_p) obeys a power law relationship with the potential scan rate (v) (i.e., $i_p = av^b$, where a and b are parameters). It can be observed from the **Figure S13b and 13d**, the b value of the 400-KOH-Ti_3C_2 electrode in 2 M H_2SO_4 solution is 0.93, which is much close to that of electrode in 2 M H_2SO_4 + 2 M $MnSO_4$ solution (b=0.92), indicating the addition of Mn^{2+} does not significantly affect the reaction kinetics of the 400-KOH-Ti_3C_2 electrode.

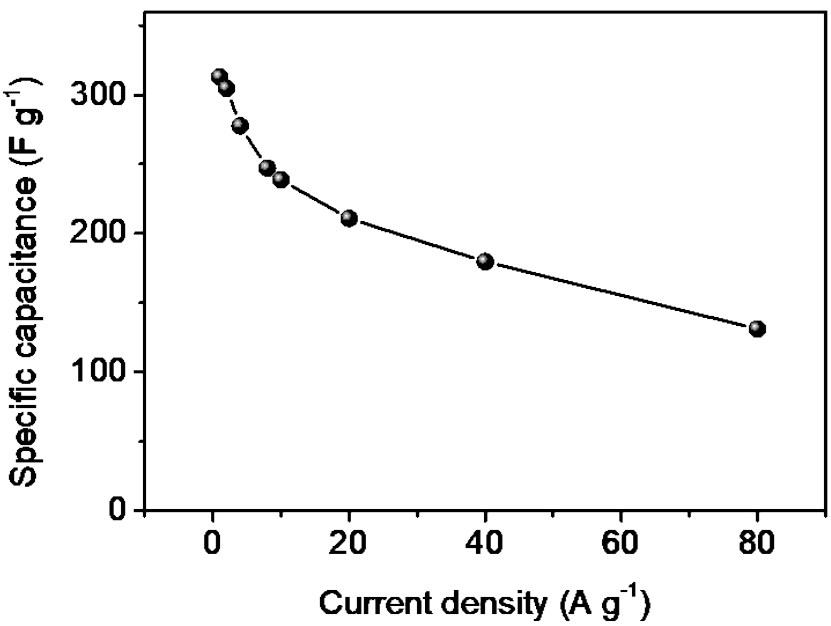

Figure S17. The specific capacitances of hybrid supercapacitor at different current densities.

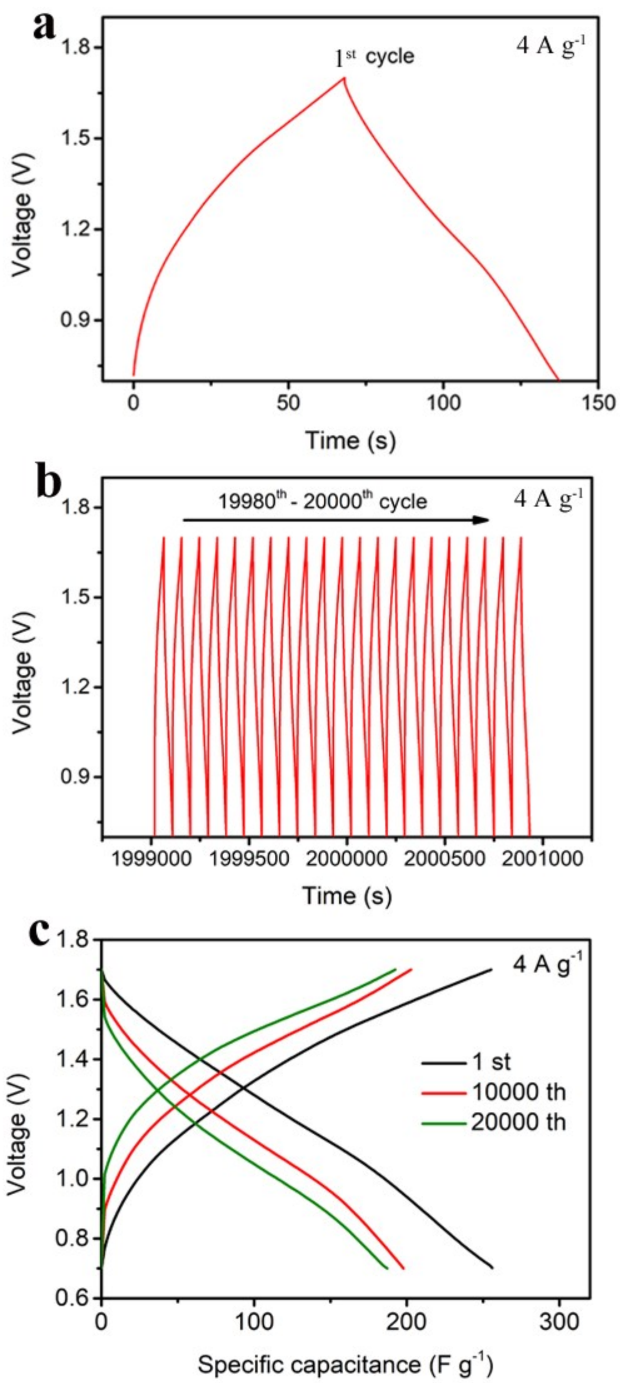

Figure S18. Galvanostatic charge/discharge curves of hybrid supercapacitor at different cycles with current density of 4 A g^{-1}.

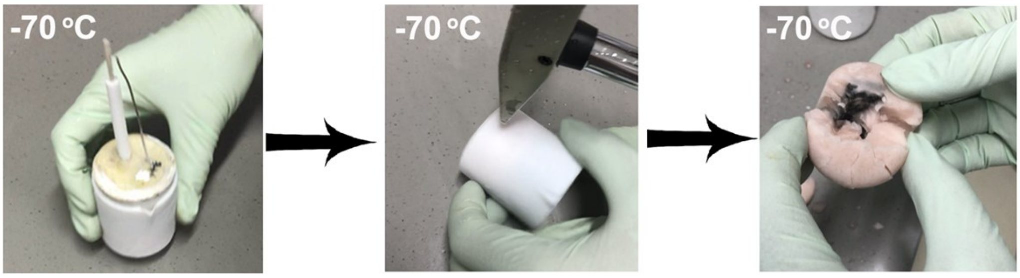

Figure S19. The photographs of the hybrid supercapacitor at -70 °C.

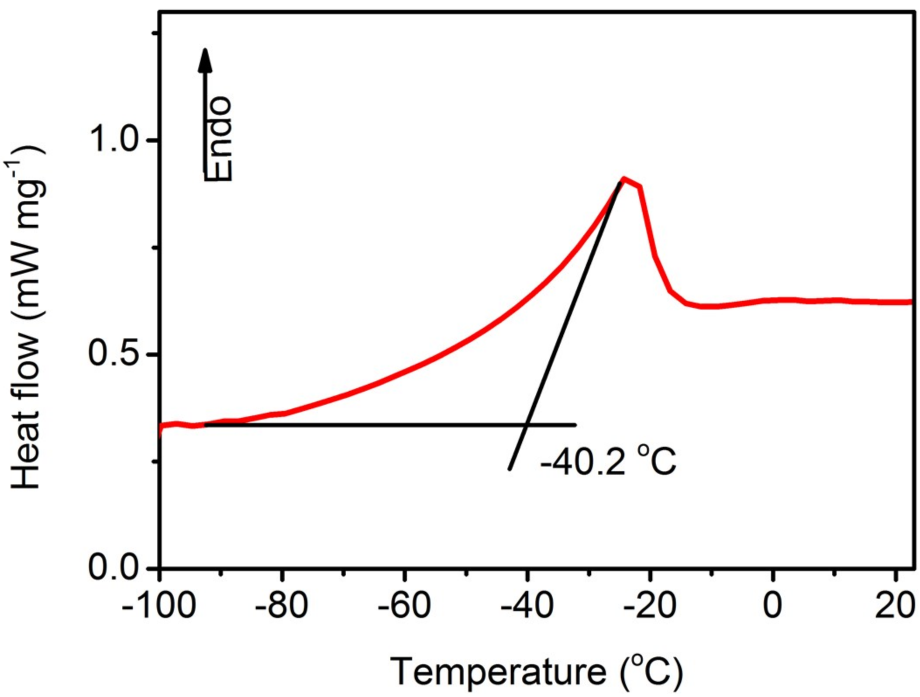

Figure S20. The DSC test for the acid electrolyte containing Mn^{2+} (2 M H_2SO_4 + 2 M $MnSO_4$).

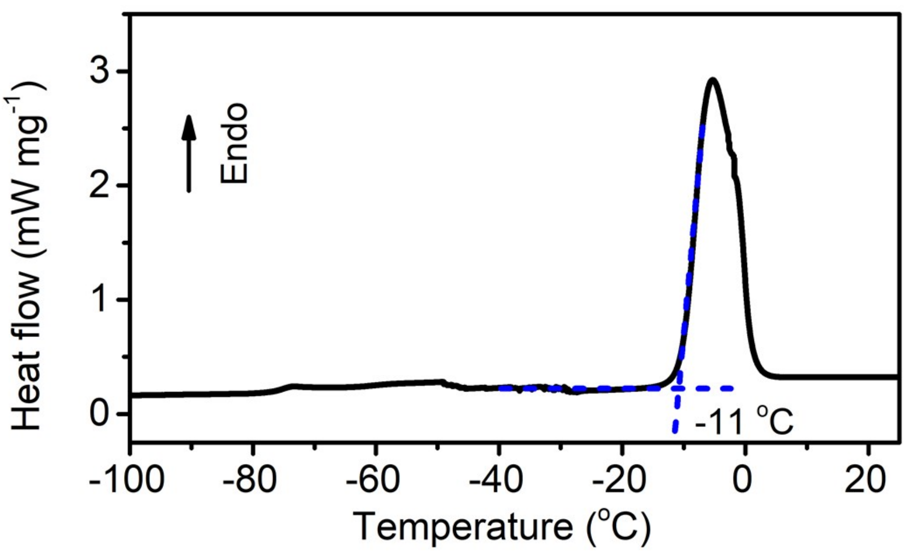

Figure S21. The DSC measurement for the 2 M $MnSO_4$ solution.

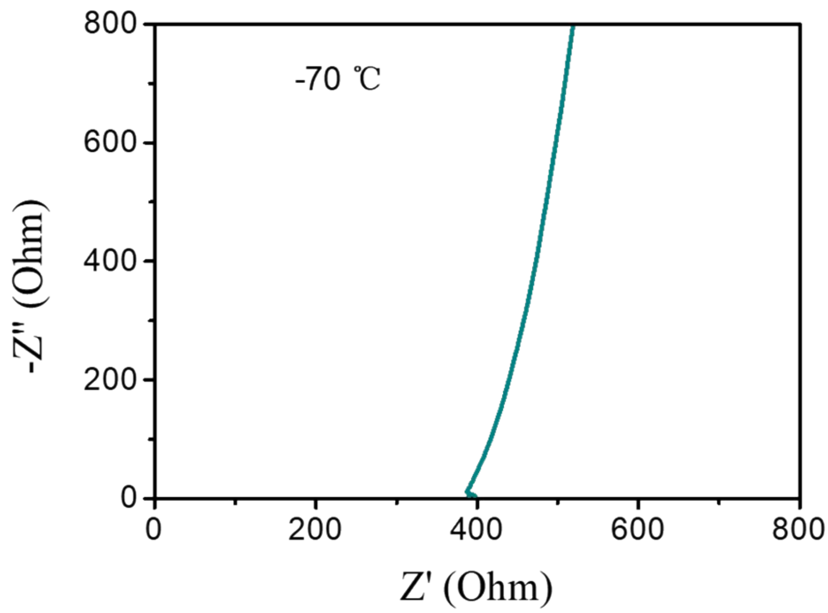

Figure S22. Nyquist plot obtained from electrochemical impedance spectroscopy investigation for the acid electrolyte containing Mn^{2+} (2 M H_2SO_4 + 2 M $MnSO_4$) at -70 ^oC.

Table S1. A comparison of the 400-KOH-Ti_3C_2 electrode with the most recently reported electrode materials using in supercapacitors about capacitance and capacitance retention.

Reference	Capacitance	Capacitance retention
6	6077 mF cm^{-2}	89.22 % (8000 cycles)
7	176 F g^{-1}	104.88 % (5000 cycles)
14	260.7 F g^{-1}	224.1 % (5000 cycles)
16	418.7 F g^{-1}	93.3 % (5000 cycles)
56	140 F g^{-1}	85 % (10000 cycles)
57	174.6 F g^{-1}	70.4 % (5000 cycles)
This work	334.5 F g^{-1}	87 % (40000 cycles)

Table S2. A comparison of the assembled hybrid supercapacitor with the most recently reported hybrid supercapacitors in terms of voltage window, capacitance and capacitance retention.

Reference	Voltage window	Capacitance	Capacitance retention
16	1.6 V	90.6 F g^{-1}	79.3 % (5000 cycles)
45	1.6 V	176 F g^{-1}	100 % (5000 cycles)
53	1.45 V	47 F g^{-1}	80 % (10000 cycles)
59	1.6 V	229.5 F g^{-1}	77 % (200 cycles)
60	1.6 V	313 F g^{-1}	137 % (50000 cycles)
61	1.3 V	72 F g^{-1}	85 % (4500 cycles)
62	1.6 V	47.59 F g^{-1}	171.75 % (6500 cycles)
63	1.4 V	3.27 F g^{-1}	135 % (7500 cycles)
64	1.6 V	221 F g^{-1}	91.83 % (10000 cycles)
This work	1.7 V	312.8 F g^{-1}	75 % (20000 cycles)

Table S3. A comparison of the assembled hybrid supercapacitor with the most recently reported hybrid supercapacitors, in terms of energy density and power density.

System	Electrolyte	Energy density	Power density
Reference 62	2 M H_2SO_4	16.92 Wh kg^{-1}	540 W kg^{-1}
Reference 66	1 M Na_2SO_4	30.4 Wh kg^{-1}	100 W kg^{-1}
Reference 67	0.5 M Na_2SO_4	19.5 Wh kg^{-1}	130 W kg^{-1}
Reference 68	1 M Na_2SO_4	22.5 Wh kg^{-1}	146.2 W kg^{-1}
Reference 69	1 M Na_2SO_4	11.3 Wh kg^{-1}	352.6 W kg^{-1}
Reference 70	1 M Na_2SO_4	40.4 Wh kg^{-1}	275 W kg^{-1}
This work	2 M H_2SO_4+2 M $MnSO_4$	43.4 Wh kg^{-1}	488.7 W kg^{-1}